IL1R8 DEFICIENCY DRIVES AUTOIMMUNITY-ASSOCIATED LYMPHOMA DEVELOPMENT

Running title: IL1R8 in autoimmunity-associated B cell lymphoma

Federica Riva[1,2], Maurilio Ponzoni[3], Domenico Supino[2], Maria Teresa Sabrina Bertilaccio[4,8], Nadia Polentarutti[2], Matteo Massara[2], Fabio Pasqualini[2], Roberta Carriero[2], Anna Innocenzi[3], Achille Anselmo[2], Tania Veliz-Rodriguez[4], Giorgia Simonetti[4,9], Hans-Joachim Anders[5], Federico Caligaris-Cappio[4,10], Alberto Mantovani[2,6,7], *Marta Muzio[4], *Cecilia Garlanda[2,6].

[1] Department of Veterinary Medicine, University of Milan, Milan, Italy.

[2] Humanitas Research Hospital, Rozzano, Italy.

[3] Ateneo Vita-Salute and Unit of Lymphoid Malignancies, IRCCS San Raffaele Scientific Institute; Pathology Unit, San Raffaele Scientific Institute, Milano, Italy.

[4] Division of Experimental Oncology, IRCCS San Raffaele Scientific Institute, Milano, Italy.

[5] Medizinische Klinik and Poliklinik IV, Klinikum der Universität München, LMU München, Germany.

[6] Humanitas University, Pieve Emanuele, Italy.

[7] The William Harvey Research Institute, Queen Mary University of London, London, United Kingdom.

[8] Present address: Department of Experimental Therapeutics, The University of Texas MD Anderson Cancer Center, Houston, Texas, USA.

[9] Present address: Biosciences Laboratory, Istituto Scientifico Romagnolo per lo Studio e la Cura dei Tumori (IRST) IRCCS, Meldola, Italy

[10] Present address: Associazione Italiana per la Ricerca sul Cancro (AIRC), Milano, Italy.

Key words: IL-1R8, autoimmunity, diffuse large B cell lymphoma, NF-kB, TLRs

Financial support: The study was supported by the European Commission (ERC project PHII-669415; FP7 project TIMER HEALTH-F4-2011-281608), Ministero dell'Istruzione, dell'Università e della Ricerca (MIUR) (project PRIN 2015YYKPNN; project FIRB RBAP11H2R9), Associazione Italiana Ricerca sul Cancro (AIRC IG 19014 to AM and AIRC 5x1000 9962 to AM and CG; AIRC IG 16777 and 13042 to MMu; AIRC 5x1000 9965 to MMu and FCC), CARIPLO (project 2010-0795 to FCC, MMu and CG), the Italian Ministry of Health (Ricerca Finalizzata, RF-2013-02355470 to CG) and the Deutsche Forschungsgemeinschaft (AN 372/24-1 and 27-1 to HJA).

* Corresponding authors:
Cecilia Garlanda
orcid.org/0000-0002-1510-7703
Humanitas Clinical and Research Center
Via Manzoni 56, 20089 Rozzano, Italy
cecilia.garlanda@humanitasresearch.it
Phone: +39 02 82255115
Fax: +39 02 82245101

or
Marta Muzio
orcid.org/0000-0002-7761-759X
IRCCS San Raffaele Hospital, Milano, Italy
Via Olgettina 60, 20132, Milano, Italy
marta.muzio@hsr.it
Phone: +39 02 26437104
Fax: +39 02 26434575

Conflict-of-interest disclosure: All the authors declare no competing financial interests.

Notes:
Text: 4769 word
Abstract: 157 words
Figures: 6
Tables: 0
References: 55

Abstract

Chronic inflammation, including that driven by autoimmunity, is associated with development of B-cell lymphomas. IL1R8 is a regulatory receptor belonging to the IL1R family, which negatively regulates NF-κB activation following stimulation of IL1R or Toll-like receptor (TLR) family members. IL1R8-deficiency is associated with the development of severe autoimmune lupus-like disease in *lpr* mice. We herein investigated whether concomitant exacerbated inflammation and autoimmunity caused by the deficiency of IL1R8 could recapitulate autoimmunity-associated lymphomagenesis. We thus monitored B-cell lymphoma development during aging of IL1R8-deficient *lpr* mice, observing increased lymphoid cell expansion that evolved to diffuse large B-cell lymphoma (DLBCL). Molecular and gene expression analysis showed that the NF-κB pathway was constitutively activated in *Il1r8*$^{-/-}$/*lpr* B splenocytes. In human DLBCL, *IL1R8* had reduced expression compared to normal B cells, and higher *IL1R8* expression was associated with better outcome. Thus, *IL1R8* silencing is associated with increased lymphoproliferation and transformation in the pathogenesis of B-cell lymphomas associated with autoimmunity.

Introduction

The association between chronic inflammation and promotion of malignancy was first described in the nineteenth century (1) and is supported by epidemiological and mechanistic data (2,3). In particular, patients suffering from certain autoimmune or inflammatory conditions, such as systemic lupus erythematosus (SLE), rheumatoid arthritis and Sjogren's syndrome are prone to develop lymphomas, namely B-cell non-Hodgkin's lymphomas (B-NHL) (4-7). The mechanisms triggering the transition from benign B-cell proliferation to malignancy are still only partially defined. Chronic inflammation, antigen stimulation and B-cell receptor signaling, associated with the inherent genetic instability of lymphocytes, are known to play a central role in lymphoma development (8,9). More specifically, gain of function mutations of MyD88 and constitutive activation of NF-κB have emerged among the most frequently recurring mutations in B-cell lymphoproliferative diseases (10).

Mice homozygous for the lymphoproliferation spontaneous inactivating mutation (*Fas*^{lpr}) show systemic autoimmunity, massive lymphadenopathy associated with proliferation of aberrant T cells, arthritis, and immune complex glomerulonephrosis (11). In humans, germline mutations in the *Fas* gene have been associated with autoimmune lymphoproliferative syndrome (ALPS) (12), and somatic *Fas* mutations have been found in multiple myeloma and B-NHL (4).

IL1R8 (also known as TIR8 or Single Ig IL1 related receptor, SIGIRR) is a member of the interleukin-1 receptor (IL1R) family acting as a negative regulatory receptor (13). IL1R8 inhibits NF-κB and JNK activation following stimulation of IL1R or TLR family members by interfering with the recruitment of TIR domain-containing adaptor molecules (14-17). In combination with IL18Rα, IL1R8 also serves as one of the receptor chains for the anti-inflammatory cytokine IL37, thereby activating anti-inflammatory responses (18).

IL1R8-deficiency leads to uncontrolled activation of IL1R or TLR family members and is associated with exacerbated inflammatory responses (14,19) and autoimmunity (16,20-22). Accordingly, downregulation of IL1R8 is observed in psoriasis (23). Depending on the context,

IL1R8 is involved in modulating either inflammation-associated tumorigenesis and tumor progression, including colorectal cancer (19,24,25) and chronic lymphocytic leukemia (CLL) (26), or NK cell–mediated antitumor immune responses in mouse models (27,28).

IL1R8-deficiency in *lpr* mice is associated with severe lymphoproliferation and autoimmune lupus-like disease (16), due to increased dendritic cell (DC) activation and B-cell proliferation in response to TLR7- and TLR9-activating autoantigens or nucleosomes (29,30).

The involvement of IL1R8 in autoimmunity, and the critical role of constitutive activation of MyD88-dependent NF-κB activation in B cell transformation raised the hypothesis that IL1R8 might be involved in the autoimmunity-associated risk of developing lymphoma. Here we show that IL1R8-deficiency was associated with significantly earlier death and increased susceptibility to lymphoproliferation, which evolved in transplantable diffuse large B-cell lymphoma (DLBCL). Analysis of clonality showed that multiple independent transformation events occurred in the same host. In humans, *IL1R8* was poorly expressed in DLBCL cell lines and primary lesions when compared to peripheral blood or germinal center B cells and was associated with better outcome in terms of overall survival, suggesting that IL-1R8 downregulation is a driver of lymphomagenesis.

Material and Methods

Animals and samples: IL1R8-deficient (*Il1r8*$^{-/-}$) mice were generated as described (14) and backcrossed to the C57BL/6J background (Charles River Laboratories, Calco, Italy) up to F11 generation. *Il1r8*$^{-/-}$ and B6*lpr/lpr* (Charles River Laboratories) were crossed to generate *Il1r8*$^{-/-}$*/lpr* mice. Mice were housed in the SPF animal facility of Humanitas Research Hospital in individually ventilated cages. Mice were sacrificed at 12-18 months of age, unless they reached the established endpoints and organs were collected for histological and molecular analysis. Procedures involving animals have been conducted in accordance with, and with the approval of the Institutional Animal Care and Use Committee (IACUC) of Humanitas Research Hospital and Italian Health Ministry (authorizations 43/2012-B released on 08/02/2012 and 828/2015-PR released on 07/08/2015), in

compliance with national (D.L. n.116, G.U., suppl. 40, February 18, 1992; D.L. n.26, March 4, 2014) and international law and policies (EEC Council Directive 86/609, OJ L 358,1,12-12-1987; EEC Council Directive 2010/63/UE; National Institutes of Health Guide for the Care and Use of Laboratory Animals, US National Research Council, 2011). All efforts were made to minimize the number of animals used and their suffering.

Histopathology and immunohistochemistry: 5 μm thick sections of formalin-fixed, paraffin embedded mouse tissues were stained with H&E. Based on lymphoid follicle morphology, a pathological score was attributed to the spleen and lymph nodes of each 10-12-month-old mouse analyzed (normal = 0; reactive = 1; reactive > atypical = 2; atypical > reactive = 3; atypical = 4; atypical > lymphomatous = 5; lymphomatous > atypical = 6; lymphomatous = 7). Slides were analyzed by a certified hematopathologist (MP) and two investigators who were blinded to the experimental group . The following antibodies were used: anti-B220 (RA3-6B2, Serotec), anti-Ki67 (SP6, Neo Markers), anti-CD3 (1F4, Biorad), anti-BCL6 (Rabbit polyclonal, Santa Cruz), anti-BCL2 (C21, Santa Cruz), anti-Multiple Myeloma 1/Interferon Regulatory Factor 4 protein (MUM1/IRF4) (3E4, Biolegend) (31).

Tumor transplantation: 10^7 cells ($5x10^6$ splenocytes plus $5x10^6$ lymph node cells) from 10-12-month-old *Il1r8*$^{-/-}$*/lpr* (n = 8) or *Il1r8*$^{+/+}$*/lpr* (n = 7) mice were injected ip, sc or iv into C57BL/6J, nude, or SCID mice (*n* = 17 recipients of *Il1r8*$^{-/-}$*/lpr* cells; *n* = 16 recipients of *Il1r8*$^{+/+}$*/lpr* cells). Recipient animals were sacrificed when clinical signs (enlargement of mandibular lymph nodes or abdomen) were evident or 12-20 months after transplantation and organs were collected for histological and molecular analysis. The genotype of several tissues of all recipient mice was analyzed for *lpr* and *Il1r8* mutations by PCR (14).

Western blot analysis of purified B-cell lysates (30 μg total proteins) was performed with the following antibodies: rabbit anti-p100/p52 (CS4882, 1:1000, o/n at 4°), mouse anti-Phospho-p65 (CS3036, 1:1000, o/n at 4°C), rabbit anti-p65 (CS8242, 1:1000, 2h RT) (Cell signaling); anti-beta-actin-HRP (SIGMA A3852, 1:10000, 2h RT), followed by anti-rabbit-HRP (Sigma A0545, 1:5000)

or anti-mouse-HRP (Sigma A3682, 1:5000), using 10% or 4-12% gradient precast gels (Genescript).

Real-Time PCR and Real-Time PCR array: Total RNA from mouse spleen purified B cells, DLBCL cell lines and B cells from healthy donor buffy coats was isolated with a column-based kit followed by DNAse treatment (Promega) (for PCR array) or TRI Reagent (Sigma-Aldrich) (for PCR). RNA was retrotranscribed and cDNA used for gene expression analysis by Real-Time PCR and Real-Time PCR array (Biorad Prime PCR ARRAY code:10034381).

Real-time PCR was performed in QuantStudium 7 Flex (Applied Biosystems, Thermo Fisher) or 7900 Sequence Detection System (Applied Biosystem), in duplicate using Power Sybr Green PCR Master Mix (Applied Biosystem) and primers (300 nM) in MicroAmp optical 96-well plates (25µl). The following primer pairs were purchased from Invitrogen: Nfkbiz for 5'-GCGCTCTCGTATGTCC-3'; Nfkbiz rev 5'-AGACTGCCGATTCCTC-3'; GAPDH for 5'-GCAAAGTGGAGATTGTTGCCAT-3'; GAPDH rev 5'-CCTTGA CTGTGCCGTTGAATTT-3' (28); human IL-1R8 For: 5'-CCGACCTTTTGG TGAACCTGA-3'; human IL-1R8 Rev: 5'-TGGCCCTCAAAGGTGATGAAG-3'; Universal actin For: 5'-CCCAAGGCCAACCGCGAGAAGAT-3'; Universal actin Rev: 5'-GTCCCGGCCAGCCAGGTCCAG-3'. Experiments were repeated at least twice. The expression of the target gene was normalized using GAPDH or β-actin cDNA expression of the same sample and run, and reported as 2^(-deltaCT).

For Real-Time PCR array, the analysis of 84 NF-κB signaling target genes was performed as described (32). Data were reported as 2^(-deltaCT), relative to the average of 6 housekeeping genes. Of note, the specific assay for Fas mRNA expression is designed within the exons 1 and 2, and it recognizes both wild type and mutant Fas (33).

IgH gene rearrangement analysis: IgH gene rearrangement was investigated by Southern blot analysis of genomic DNA from different organs of one 20-month-old wild-type mouse transplanted sc with total lymph node and spleen cells collected form one 11-month-old *Il1r8*$^{-/-}$*/lpr* mouse. DNA

(5 μg) was extracted from spleen, lymph nodes, and solid lesions (100 mg each), digested with EcoRI or StuI and subsequently hybridized with a ^{32}P-labeled DNA probe PJ3 representing the JH4 region of the IgH locus, as described (34).

Cell culture: B cells were isolated from 100x10^6 splenocytes using a B cell isolation kit (Miltenyi Biotec), plated in 48-well plate at 1 x 10^6/ml and cultured overnight.

Human DLBCL cell lines SU-DHL-2 (ATCC CRL-2956), SU-DHL-4 (ATCC CRL-2957), SU-DHL-6 (ATCC CRL-2959), SU-DHL-8 (ATCC CRL-2961), RC-K8 (DSMZ ACC-561), and RIVA (RI-1; DSMZ ACC-585) were received in 2013, expanded and frozen, and then thawed and grown for 10 days in RPMI or IMDM (RIVA, RC-K8) medium supplemented with 10–20% FCS, 2mM L-glutamine, and streptomycin (100 U/ml) before the experiments. DLBCL cell lines were not authenticated, were routinely tested for Mycoplasma contamination and only Mycoplasma free cells were used for flow cytometry and molecular analysis.

Flow cytometric analysis: Mouse spleen B cells overnight cultured in medium or in presence of LPS (100 ng-1 μg/ml, Sigma-Aldrich) were incubated with anti-mouse CD86 (GL1, eBioscience) and anti-mouse CD19 (1D3, BD Bioscience) for 30 min at 4°C for surface staining and analyzed by FACS canto II (Becton Dickinson, Franklin Lakes, NJ, USA).

IL1R8 cell surface staining on human cells was performed with biotinylated goat anti-human IL1R8/SIGIRR (R&D Systems), followed by Alexa-647 conjugated streptavidin (Molecular Probes, Invitrogen), and analyzed with FACS Canto I flow cytometer (BD Bioscience). Results are reported as mean fluorescence intensity (MFI) normalized on fluorescence minus one. Diva software (BD Pharmingen) and Flow-jo (Tree Star) were used for data acquisition and analysis, respectively.

Analysis of IL1R8 and IL37 expression in human DLBCL: Public gene expression data of DLBCL were retrieved from GEO. In the first study (GSE43677) samples of naïve B cells (n = 8), germinal center (GC) B cells (n = 13), post-GC B cells (n = 9), tonsils (n = 10), and DLBCL (n = 12) were analyzed. In the second study (GSE32018) gene expression profiling was conducted in a series of B-cell non-Hodgkin lymphoma patients (17 CLL, 22 DLBCL, 23 Follicular Lymphoma

(FL), 24 Mantle Cell Lymphoma (MCL), 15 marginal zone lymphoma-MALT type (MALT), 13 Nodal Marginal Zone Lymphoma (NMZL)), and 7 freshly frozen lymph nodes. Differential expression analysis was performed using limma (version 3.26.8) (35). For prognosis evaluation, expression and clinical data of 98 DLBCL cases selected from 220 lymphoma samples (GSE4475) were used. DLBCL patients treated with radiotherapy were excluded.

The Gene Set Enrichment Analysis (GSEA) software was used to perform the over-representation analysis with gene sets coming from the Molecular Signature Database (36). The entire datamatrix containing normalized gene expression values (log-scale) was used, and the expression profile of IL1R8 gene was tested as continuous phenotype label. The analysis was performed choosing the Pearson correlation as the metric to investigate gene sets enriched by genes correlated with the expression profile of IL1R8. The Reactome database, belonging to the C2 collection (c2.cp.reactome.v6.1), was used. Resulting gene sets were considered significantly enriched according to the False Discovery Rate (FDR) threshold of 5%.

Statistical analysis: Statistical differences in mouse mortality and lymphoma incidence rates were analyzed with Mantel-Cox test and Fisher test, respectively. Mann Whitney test or Student *t* test with Welch's correction were performed as specified. Survival analysis of human DLBCL was performed using Kaplan-Meier and Mantel-Cox tests. The median gene expression value was used to classify patients into $IL1R8^{low}$ and $IL1R8^{high}$ or $IL37^{low}$ and $IL37^{high}$ gene expression groups. A P value < 0.05 was considered statistically significant. Statistical analysis was performed using Graph Pad Prism software (Graph Pad Software, San Diego, CA).

Results

IL1R8-deficiency is associated with severe lymphadenopathy and lymphoma in *lpr* mice

We previously observed that 6-month-old *Il1r8*$^{-/-}$*/lpr* mice were affected by enhanced lymphoproliferation and lymph follicle hyperplasia compared to *Il1r8*$^{+/+}$*/lpr* mice (16). In order to address whether this benign lymphoproliferation eventually evolved to malignancy, we analyzed

survival and followed the evolution of lymphoid organs in older animals. As shown by survival curves reported in Fig. 1A, *Il1r8*$^{-/-}$*/lpr* mice reached the endpoints earlier than *Il1r8*$^{+/+}$*/lpr* mice, and mortality was 100% (23/23) at 15 months of age in *Il1r8*$^{-/-}$*/lpr* mice compared to 22% (6/27) in *Il1r8*$^{+/+}$*/lpr* mice (P = 0.0001, Mantel-Cox test). Splenomegaly and lymphadenomegaly were more pronounced in 10-12-month-old *Il1r8*$^{-/-}$*/lpr* mice compared to *Il1r8*$^{+/+}$*/lpr* mice of the same age (Fig. 1B). The spleen weight was significantly increased in both groups compared to wild type or *Il1r8*$^{-/-}$ mice, and in *Il1r8*$^{-/-}$*/lpr* mice it was significantly greater (4-fold) than in *Il1r8*$^{+/+}$*/lpr* mice (Fig. 1C).

Histopathological analysis of the spleens of 12-14-month-old *Il1r8*$^{-/-}$*/lpr* mice showed an enlargement of the white pulp and a complete loss of the normal architecture of the organ in most animals (Fig. 2A). In the spleens of 12-14-month-old *Il1r8*$^{+/+}$*/lpr* mice, we observed a moderate enlargement of the white pulp, but the architecture of the organ remained recognizable despite the presence of enlarged germinal centers (Fig. 2A). Similarly, most (62.5%; 20/32) lymph nodes from 10-12-month-old *Il1r8*$^{-/-}$*/lpr* mice presented abnormal histological architecture, without any evident follicle (Fig. 2B). In contrast, lymph nodes from 10-12-month-old *Il1r8*$^{+/+}$*/lpr* mice were enlarged but generally retained a preserved normal morphology of the follicles (Fig. 2B). As shown in Fig. 2C and 2D, the pathological score of lymphoid follicles (based on the presence of normal, reactive, atypical, or lymphomatous follicles) was significantly higher in 10-12-month-old *Il1r8*$^{-/-}$*/lpr* mice compared to 12-14-month-old *Il1r8*$^{+/+}$*/lpr* mice (p = 0.0001 in spleen and p = 0.0022 in lymph nodes), and the diagnosis of lymphoma was mostly limited to *Il1r8*$^{-/-}$*/lpr* mice. Splenic and lymph nodal plasmacytosis occurred in spleen and lymph nodes of both *Il1r8*$^{+/+}$*/lpr* and *Il1r8*$^{-/-}$*/lpr* mice, in agreement with the role of TLR ligands and autoantigens in inducing cellular differentiation into mature plasma cells and plasma cell expansion (37,38).

Development of Diffuse Large B Cell Lymphoma in *Il1r8*$^{-/-}$*/lpr* mice

Histopathological analysis showed that a diffuse organ replacement by large cells in spleen and lymph nodes consistent with a diagnosis of lymphoma occurred in 13/26 *Il1r8*$^{-/-}$*/lpr* mice and 3/23 *Il1r8*$^{+/+}$*/lpr* mice (P = 0.0073, Fisher test) (Fig. 2E). In 8 out of 13 mice with lymphoma (61.5%), large cells were observed in liver, lung, kidney, and gut, indicating the development of Diffuse Large B Cell Lymphoma (DLBCL). Immunostaining for B220 highlighted a diffuse infiltration by large neoplastic B cells (Fig. 3A). CD3^{+} T cells appeared distributed throughout the tissue, rather than clustering within and around follicles of the splenic white pulp in lymphoma-bearing *Il1r8*$^{-/-}$*/lpr* mice (Fig. 3B). Neoplastic B lymphocytes were relatively monomorphic, with large nuclei and abundant cytoplasm; within this population, high mitotic rate as well as diffusely elevated Ki67 immunoreactivity confirmed the increased proliferation rate of these lymphomas (Fig. 3C). In addition, neoplastic B cells were immunoreactive for Bcl-2, suggesting an activation of an anti-apoptotic machinery, and negative for Bcl-6 and MUM1 (Fig. 3D, 3E, and 3F, respectively). In *Il1r8*$^{-/-}$*/lpr* lymph nodes, we observed lesions with similar features and in a few cases (3/13, 23%), bone marrow of *Il1r8*$^{-/-}$*/lpr* mice showed small and focal areas of DLBCL.

DLBCL was rarely diagnosed in *Il1r8*$^{+/+}$*/lpr* mice older than 12 months (3/23, 13 %) as well, . The vast majority of *Il1r8*$^{+/+}$*/lpr* old mice actually showed an irregular enlargement of germinal centers with predominance of intermediate cells, without fulfilling the required criteria for follicular lymphoma. In addition, the presence of few, scattered large B220^{+} cells was consistent with atypical, lymphoproliferative, potentially pre-neoplastic disorder (Fig. 3A, 3B, and 3C).

Il1r8$^{-/-}$*/lpr* DLBCL are transplantable and oligoclonal

In order to further demonstrate the malignant capability of lesions developing in aged *Il1r8*$^{-/-}$*/lpr* and *Il1r8*$^{+/+}$*/lpr* mice, splenocytes and lymph node cells collected from eight and seven donors, respectively, were injected through different routes in immunodeficient (nude and SCID) or immunocompetent mice (17 recipients of *Il1r8*$^{-/-}$*/lpr* and 16 recipients of *Il1r8*$^{+/+}$*/lpr* cells). Irrespective of the immunocompetence of the recipient mouse and route of injection, after 4-20

months of observation, cells from 4/ 8 *Il1r8*$^{-/-}$*/lpr* mice generated histologically-confirmed parental DLBCL in recipient mice (Fig. 4A). In contrast, mice injected with cells collected from the seven *Il1r8*$^{+/+}$*/lpr* donor mice did not develop lymphoma in recipient mice up to 20 months of observation. Genotyping for *lpr* and *Il1r8* gene modifications was performed by PCR analysis on genomic DNA of several tissues of all recipient mice. Genotyping of the recipient's organs affected by lymphoma (spleen, lymph nodes) and control tissues (skeletal muscle) confirmed that malignant cells originated from the *Il1r8*$^{-/-}$*/lpr* donors (Fig. 4B).

Since lymphoma lesions infiltrated more than one lymphoid organ in *Il1r8*$^{-/-}$*/lpr* mice, we next assessed whether these lesions originated from a common B cell clone. Southern blot analysis was performed to detect immunoglobulin (Ig) heavy chain gene (IgH) rearrangements in DLBCL developed in different organs of one recipient wild-type mouse transplanted with splenocytes and lymph node cells of one *Il1r8*$^{-/-}$*/lpr* donor. The analysis revealed bands of IgH rearrangement of different size in the spleen, lymph nodes and other organs indicating that multiple B cell clones were transformed in the donor mouse (Fig. 4C-D).

These results indicate that lymphomas of *Il1r8*$^{-/-}$*/lpr* mice can be transplanted in wild-type recipient mice giving rise to lymphoma.

Constitutive activation of the NF-κB pathway in *Il1r8*$^{-/-}$*/lpr* B cells

Hyper-activation of the NF-κB pathways and overexpression of NFKBIZ are hallmarks of a subtype of Diffuse Large B-cell lymphoma in humans (39-41). IL1R8 dampens NF-κB activation induced by TLR and IL1R family members (42), and Fas mutations impact B-cell activation (16). In addition, we previously showed that IL1R8-deficiency significantly increased B-cell proliferation upon exposure to RNA and DNA immune complexes and other TLR agonists (16). To further investigate the NF-κB pathway in B cells of *Il1r8*$^{-/-}$*/lpr* old mice, we analyzed NF-κB activation and the expression of specific NF-κB regulated genes in CD19^{+} cells purified from the spleen of 12-month-old *Il1r8*$^{+/+}$, *Il1r8*$^{-/-}$, *Il1r8*$^{+/+}$*/lpr* and *Il1r8*$^{-/-}$*/lpr* mice, in resting conditions or after

316 stimulation with LPS. Noncanonical and canonical NF-κB activation can be monitored by the
317 cleavage of p100 (Nfkb2) into p52 fragment, and phosphorylation of p65 (RelA), respectively. In
318 contrast to wild type mice, we observed activation of noncanonical NF-κB pathway in both
319 *Il1r8*$^{+/+}$*/lpr* and *Il1r8*$^{-/-}$*/lpr* mice, whereas the canonical pathway appeared mostly activated in the
320 *Il1r8*$^{+/+}$*/lpr* mice (Fig. 5A–C). We did not observe any significant difference in *Il1r8*$^{-/-}$ mice at this
321 time point compared to *Il1r8*$^{+/+}$mice in the absence of *ex vivo* stimulation.

322 Next, we used real-time PCR array to analyze 84 genes known to be targets of the NF-κB
323 signaling pathway (Supplementary Table S1). We compared the results obtained from non-
324 stimulated B cells collected from 4 wild type mice, 4 *Il1r8*$^{-/-}$ mice, 5 *Il1r8*$^{+/+}$*/lpr* mice, and 5 *Il1r8*$^{-/-}$
325 */lpr* mice (Fig. 5D and Supplementary Table S2). Of the 14 genes dysregulated in at least one
326 group, 13 genes were upregulated, and only one was downregulated as compared to wild type
327 animals, again suggesting constitutive hyperactivation of this pathway in *Il1r8*$^{+/+}$*/lpr* and *Il1r8*$^{-/-}$*/lpr*
328 B cells from aged mice. Most of the NF-κB targets were upregulated in both *Il1r8*$^{+/+}$*/lpr* and *Il1r8*$^{-/-}$
329 */lpr* mice, including proinflammatory genes (e.g. *Il1b*, *Ifng*, *Csf1*, *Stat1*, *Il12b*) and genes associated
330 with proliferation or anti-apoptosis (e.g. *Ccnd1*) (Supplementary Table S2). The *Bcl2a1a* gene
331 coding for an anti-apoptotic protein necessary for cell transformation and growth in anaplastic
332 lymphoma (43) was downregulated in *lpr* mice (fold difference = 0.47 and p = 0.04 as shown in
333 Supplementary Table S2), and although IL1R8 deficiency did not influence its expression (fold
334 difference = 0.93; p = 0.8), expression was restored in *Il1r8*$^{-/-}$*/lpr* mice (fold difference = 1.08 and p
335 = 0.8 as shown in Supplementary Table S2).

336 We then analyzed a secondary response gene prototypically induced by TLRs and regulated
337 by NF-κB, namely *Nfkbiz*. In basal conditions we observed low expression of *Nfkbiz* mRNA in B
338 cells isolated from wild type mice; however, *Nfkbiz* was significantly induced in *Il1r8*$^{-/-}$ mice, and
339 this induction was sustained in *Il1r8*$^{-/-}$*/lpr* mice (Fig. 5E), suggesting that a TLR-dependent NF-κB
340 secondary response is constitutively activated in *Il1r8*$^{-/-}$ *and Il1r8*$^{-/-}$*/lpr* mice.

In agreement with dysregulated activation of the NF-κB pathway, flow cytometry analysis showed that overnight-cultured, spleen-purified *Il1r8*$^{-/-}$*/lpr* B cells had increased expression of CD86, an activation marker downstream of TLR activation (44,45), compared to wild type, *Il1r8*$^{-/-}$ and *Il1r8*$^{+/+}$*/lpr* B cells, both in basal conditions and after LPS stimulation (Fig. 5F).

Taken together, these results show that both Fas- and IL1R8-deficiency contribute to constitutive dysregulated NF-κB signaling and increased B cell activation with few differences associated with IL1R8 deficiency (e.g. induction of *Nfkbiz*) . The double mutation rendered the cells highly responsive to TLR activation, as measured by CD86 expression.

IL1R8 expression is downmodulated in human DLBCL cells and correlates with prognosis

To assess the relevance of these results to human disease, we first studied the expression of IL1R8 in human lymphoma cell lines compared with normal circulating mature B cells. As shown in Fig. 6A and B, all DLBCL cell lines analyzed expressed lower IL1R8 mRNA and protein, respectively, compared to peripheral blood B cells.

Next, we studied IL1R8 expression in public gene expression data of DLBCL retrieved from GEO, comparing different normal resting and activated B cell populations and lymphomas. In the first study analyzed (GSE43677), the expression of IL1R8 was significantly down-regulated in DLBCL samples *vs* naive B cells (logFC = -0.43, Adj. *P*-value = 1.08E-04), GC B cells (logFC = -0.21, Adj. *P*-value = 1.70E-02), post-GC B cells (logFC = -0.9, Adj *P*-value = 1.12E-09), and tonsils (logFC = -0.62, Adj. *P*-value = 3.64E-08) (Fig. 6C). The second study (GSE32018) showed a significant down-regulation of IL1R8 expression in DLBCL *vs* lymph node control samples (logFC = -1.34, Adj. *P*-value = 1.65E-02), but also *vs* FL, an indolent form that may transform into DLBCL (logFC = -0.66, Adj. *P*-value = 3.45E-02) (Fig. 6D).

In a third study (GSE4475), the expression of IL1R8 was analyzed together with clinical data to evaluate a correlation with prognosis. DLBCL patients were divided into IL1R8^{low} and IL1R8^{high} based on the median gene expression. The resulting Kaplan-Meier curve showed that

patients with IL1R8 expression above the median value had significantly prolonged overall survival (Hazard Ratio (HR) = 2.2 (95% C.I. 1.2-3.8); *P*-value = 0.006) (Fig. 6E), compared with patients below the median. In addition, the GSEA analysis retrieved a total of 60 pathways significantly enriched by genes positively correlated with IL1R8 gene expression profile (Supplementary Table S3). Among these, the apoptotic process and the DNA damage response were two of the most enriched pathways (NES = 2.02, FDR q-val = 0.005 for the apoptosis process; NES = 1.85, FDR q-val = 0.01 for the P53-dependent G1 DNA damage response) with a total of 70 and 29 genes, respectively, belonging to the core enrichment (Supplementary Table S4 and Table S5). These results show a positive coregulation of apoptotic process and DNA damage response genes with our gene of interest, suggesting a putative activation of the apoptotic process and DNA damage response in profiles with high IL1R8 expression compared to those with low expression.

Since IL1R8 is required for the anti-inflammatory activity of IL37 in inflammatory conditions triggered by TLR ligands (18,46), we finally investigated whether IL1R8 and IL37 were coregulated in DLBCL. In the GSE43677 and GSE32018 studies, the expression of IL37 was significantly down-regulated in DLBCL samples compared to normal B cells (logFC = -0.18, Adj. *P*-value = 3.73E-02 for naïve B cells, logFC = -0.25, Adj. *P*-value = 1.65E-03 for GC B cells) or FL cells (logFC = -0.37, Adj. *P*-value = 4.30E-03), respectively, similarly to IL1R8. However, in contrast to what was observed for IL1R8, the overall survival was not affected by IL37 expression in the GSE4475 study (HR = 0.6 (95% C.I. 0.4-1.1); *P*-value = 0.1), indicating that the regulatory role of IL1R8 impacts additional pathways.

These results indicate that IL1R8 is poorly expressed in DLBCL compared to healthy GC B cells and other B cell lymphomas, and that lower IL1R8 expression is associated with shorter overall survival.

Discussion

IL1R8 is known to act as a negative regulator of NF-κB and JNK activation following stimulation of IL1R family members or TLRs. We herein showed that the increased susceptibility to lymphoproliferation observed in *lpr* mice deficient of IL1R8 is also associated with frequent development of DLBCL. The aggressive lymphomas that developed in *Il1r8*$^{-/-}$*/lpr* mice were transplantable and oligoclonal, possibly originating from multiple B cell clones. In addition, we showed that IL1R8 expression is down-regulated in human DLBCL cells in comparison with peripheral blood, GC B cells, and other lymphomas. Expression also correlated with overall survival, suggesting that IL1R8 silencing in DLBCL might contribute to dysregulated NF-κB activation, a frequent occurrence observed in DLBCL, lymphoproliferation, and transformation.

FAS-deficient *lpr* mice are a model of ALPS and SLE. FAS is a pro-apoptotic TNF receptor superfamily member, highly expressed on GC B cells. Mutations in the genes encoding FAS or its ligand (FASL) cause massive accumulation of autoreactive B and T cells, resulting in ALPS in humans (12). In addition, FAS mutation has been found associated with perforin deficiency in one case of ALPS and lymphoma (47), whereas in mice, increased lymphoma development was observed in *lpr* mice deficient of SPARC, the gene coding for osteonectin (48). In a previous study, we demonstrated that IL1R8-deficiency was associated with a more severe lymphadenopathy at 6 months of age in FAS-deficient *lpr* mice (16). This phenotype was mainly due to overactivation of DCs, B cells, and $CD4^+$ T cells upon stimulation with lupus autoantigens, possibly through TLR7 engagement (16). Indeed, chromatin antigens in immune complexes can potently engage both the BCR and TLRs in B cells, leading to overstimulation and defective apoptosis of B cells, as well as to secondary inflammation (5). FAS mutations have also been observed in human lymphomas, indicating that longer lymphocyte survival may allow accumulation of additional oncogenic events (4).

In addition to these autoimmunity-dependent mechanisms, genetic alterations affecting components of the NF-κB signaling pathways have been shown to occur frequently in DLBCL. Constitutive NF-κB pathway activity is observed in almost all activated B cell–like (ABC) types of

DLBCL and in a large fraction of germinal center B cell (GCB)–DLBCLs, and is associated with proliferation, differentiation, and survival of malignant lymphoid cells (49,50). Among mutations of the NF-κB signaling pathway in B cell lymphomas, MYD88 mutations have emerged as one of the most frequently recurring (40). MyD88 is an adaptor protein that mediates TLR and IL1R signaling. Gain of function mutations of MYD88 confer a cell survival advantage during evolution of DLBCL by promoting NF-κB and JAK/STAT3 signaling (40). IL1R8 tunes TLR and IL1R-dependent signaling by interfering with the recruitment of TIR-containing adaptor molecules (51) and IL1R8-deficiency in mice is associated with uncontrolled inflammatory responses both in infectious and sterile conditions (42). Furthermore, genetic inactivation of IL1R8 was observed to cause earlier, more disseminated, and aggressive leukemia in the Eμ-TCL1 mouse model of CLL (26). In this model, the neoplastic transformation of B cells has an incidence of 100% and is mediated by the overexpression of the TCL1 oncogene; the absence of IL1R8 exacerbates CLL progression, but its impact on the B cell transformation has not been investigated (26). Finally, IL1R8 in association with IL18Rα serves a receptor chain for IL37, a cytokine which provides an anti-inflammatory environment in the aging bone marrow, preventing oncogenic transformation of B cell progenitors (52). Our results show that *Il1r8*$^{+/+}$*/lpr* mice spontaneously developed DLBCL at a very low frequency and at late age (12–18 months). IL1R8-deficiency increased the frequency and the severity of the disease, as well as accelerated the onset of disease to 8-12 months of age, indicating that IL1R8 has also a role in neoplastic transformation of B cells, and not only in the progression of established B-cell leukemia or lymphoma.

The pathogenesis of lymphoma seen in patients with autoimmune diseases is complex and involves different factors contributing to lymphomagenesis, including both disease activity and immunosuppression, as well as disease-specific mechanisms and mechanisms unique to lymphoma subtype (8). In the current study, we show that the *Il1r8*$^{-/-}$*/lpr* mouse model recapitulated autoimmunity-associated lymphomagenesis, suggesting that the absence of a negative regulator of the ILR- or TLR-MyD88 axis in an autoimmune-prone background is sufficient for the neoplastic

transformation of B cells. These results are in line with data in humans, showing that aggressive B-cell lymphomas (particularly DLBCL) are more frequently associated with autoimmune conditions than more indolent lymphomas (particularly FL) (4). It should be noted that IL1R8-deficiency in this model was not restricted to B cells and might also impact on antitumor immunity, as shown in other models (27,28). Therefore, our results may underestimate the effect of selective IL1R8-deficiency in tumor B cells.

Western blot analysis of p52 and phospho-p65 demonstrated that both canonical and non-canonical NF-κB pathways are constitutively activated in *Il1r8*$^{+/+}$*/lpr* mice. Moreover, the TLR-induced NF-κB-regulated Nfkbiz gene was constitutively activated in *Il1r8*$^{-/-}$ mice. A combination of these pathways may contribute to the activation of distinct NF-κB target genes and B-cell activation observed in lymphoma prone *Il1r8*$^{-/-}$*/lpr* mice. We previously observed that *Il1r8*$^{-/-}$*/lpr* B cells had increased proliferation rate after stimulations with autoantigens acting through TLR7, TLR9, and other TLR ligands, compared to *lpr* B cells (16). In the present manuscript, we described a high mitotic rate and diffusely elevated Ki67 immunoreactivity in *Il1r8*$^{-/-}$*/lpr* spleen, indicating increased proliferation rate, associated with immunoreactivity for Bcl-2, suggesting activation of antiapoptotic machinery. Thus, the results presented here are in line with the view that the lack of a tuner of TLR and IL1R signaling–dependent NF-κB activation could impinge upon B cell transformation in the context of lymphoproliferative syndrome. Indeed, other oncogenic events circumventing negative feedback mechanisms that attenuate NF-κB signaling, such as inactivation of the deubiquitinase A20, are associated with autoimmunity and lymphoma development (40,53).

DLBCLs developed in *Il1r8*$^{-/-}$*/lpr* mice were characterized by the presence of a monomorphic population of large B cells in lymphoid tissues. Neoplastic B cells displayed high proliferation rates and showed widespread involvement of distant organs including gut, liver, lung, and kidney. Histopathologic analysis and immunostaining for CD3, B220, Bcl-2, and Ki67 of spleen and lymph node specimens of *Il1r8*$^{-/-}$*/lpr* mice documented sharply separated masses constituted by DLBCL arising within a background characterized by atypical lymphoproliferative

disorder. Excessive lymphoproliferation associated with activation of anti-apoptotic mechanisms were potentially responsible for multiple independent transformation events resulting in polyclonal (or oligoclonal) development of different primary foci of DLBCL, as suggested by the detection of different bands of IgH rearrangement in the same mouse or in the same organ. Our results suggest that FAS-deficiency was responsible for polyclonal B-cell expansion and very rarely lymphoma transformation, and the addition of the deficiency of IL1R8 causing hyperactivation of the MyD88-NF-κB axis, in response to autoantigens, resulted in tumors that resemble human ABC-DLBCL. In *Il1r8*$^{-/-}$*/lpr* mice, these tumors emerged sporadically and thus were likely to have acquired the additional oncogenic hits necessary to give rise to DLBCL.

In the present study, we show that the expression of IL1R8 in human DLBCL was downmodulated compared to peripheral blood or GC B cells from healthy donors and correlated with overall survival. The molecular mechanisms underlying IL1R8 downmodulation in human DLBCL are still undefined, and could include promoter methylation, as observed in human gastric carcinomas (54), alternative splicing leading to aberrant protein expression, as described in colorectal cancer (55), or promoter hypo-acetylation as suggested by the analysis of hematological cancer cell lines from public available datasets (Ensembl, UCSC Genome Browser). In addition, it was reported that genomic methylation affects IL1R8 expression, as Azacytidine treatment of CLL cell lines restored IL1R8 mRNA expression (56). Very rarely, nonsense and somatic non-synonymous mutations have been observed in IL1R8 coding sequence as shown by Whole Exome Sequencing data from The Cancer Genome Atlas (TCGA) and in sequenced samples within DLBCL patients (Dalla-Favera R., personal communication), but the functional consequences of these mutations or polymorphisms need to be investigated. The apoptotic process and DNA damage response were among the pathways significantly enriched by genes positively correlated with IL1R8 gene expression. This suggests that higher IL1R8 expression might be associated with increased apoptotic activity and better control of DNA damage, and as a consequence, with a less aggressive phenotype of lymphoma cells, thus leading to better prognosis.

Patients affected by DLBCL show different clinical courses, making prediction of prognosis and successful therapy difficult, leading to only 50% of patients being effectively treated (57). Our results demonstrate that IL1R8 activity limits B-cell activation and malignant transformation induced by autoimmune stimulation and contribute to the identification of genes and molecular pathways that could represent targets for novel therapeutic approaches in DLBCL treatment.

Supplemental material includes Supplementary Table S1, S2, S3, S4, S5.

Authorship

Contribution: F.R, F.C-C., A.M, M.Mu., and C.G. conceived the study; F.R., M.P., D.S., S.B., M.Ma., A.I., H.J.A. and M.Mu. designed and/or conducted experiments, performed data analysis and interpretation, and informed study direction; F.P., N.P., A.A., T.V-R., and G.S. helped with experimental work; R.C. performed bioinformatics analyses; F.R., M.Mu. and C.G. drafted the manuscript; and all authors discussed the results and commented on the manuscript.

References

1. Mantovani A, Allavena P, Sica A, Balkwill F. Cancer-related inflammation. Nature **2008**;454(7203):436-44.

2. Balkwill F, Charles KA, Mantovani A. Smoldering and polarized inflammation in the initiation and promotion of malignant disease. Cancer Cell **2005**;7(3):211-7.

3. Coussens LM, Zitvogel L, Palucka AK. Neutralizing tumor-promoting chronic inflammation: a magic bullet? Science **2013**;339(6117):286-91 doi 10.1126/science.1232227.

4. Gronbaek K, Straten PT, Ralfkiaer E, Ahrenkiel V, Andersen MK, Hansen NE, *et al.* Somatic Fas mutations in non-Hodgkin's lymphoma: association with extranodal disease and autoimmunity. Blood **1998**;92(9):3018-24.

5. Dias C, Isenberg DA. Susceptibility of patients with rheumatic diseases to B-cell non-Hodgkin lymphoma. Nat Rev Rheumatol **2011**;7(6):360-8 doi 10.1038/nrrheum.2011.62.

6. Poppema S, Maggio E, van den Berg A. Development of lymphoma in Autoimmune Lymphoproliferative Syndrome (ALPS) and its relationship to Fas gene mutations. Leuk Lymphoma **2004**;45(3):423-31.

7. Carbone A, Tripodo C, Carlo-Stella C, Santoro A, Gloghini A. The role of inflammation in lymphoma. Adv Exp Med Biol **2014**;816:315-33 doi 10.1007/978-3-0348-0837-8_12.

8. Baecklund E, Smedby KE, Sutton LA, Askling J, Rosenquist R. Lymphoma development in patients with autoimmune and inflammatory disorders--what are the driving forces? Semin Cancer Biol **2014**;24:61-70 doi 10.1016/j.semcancer.2013.12.001.

9. Shaffer AL, Rosenwald A, Staudt LM. Lymphoid malignancies: the dark side of B-cell differentiation. Nat Rev Immunol **2002**;2(12):920-32 doi 10.1038/nri953.

10. Pasqualucci L, Dalla-Favera R. The genetic landscape of diffuse large B-cell lymphoma. Semin Hematol **2015**;52(2):67-76 doi 10.1053/j.seminhematol.2015.01.005.

11. Singer GG, Carrera AC, Marshak-Rothstein A, Martinez C, Abbas AK. Apoptosis, Fas and systemic autoimmunity: the MRL-lpr/lpr model. Curr Opin Immunol **1994**;6(6):913-20.

12. Fisher GH, Rosenberg FJ, Straus SE, Dale JK, Middleton LA, Lin AY, *et al.* Dominant interfering Fas gene mutations impair apoptosis in a human autoimmune lymphoproliferative syndrome. Cell **1995**;81(6):935-46.

13. Garlanda C, Dinarello CA, Mantovani A. The interleukin-1 family: back to the future. Immunity **2013**;39(6):1003-18 doi 10.1016/j.immuni.2013.11.010.

14. Garlanda C, Riva F, Polentarutti N, Buracchi C, Sironi M, De Bortoli M, *et al.* Intestinal inflammation in mice deficient in Tir8, an inhibitory member of the IL-1 receptor family. Proc Natl Acad Sci U S A **2004**;101(10):3522-6.

15. Wald D, Qin J, Zhao Z, Qian Y, Naramura M, Tian L, *et al.* SIGIRR, a negative regulator of Toll-like receptor-interleukin 1 receptor signaling. Nat Immunol **2003**;4(9):920-7.

16. Lech M, Kulkarni OP, Pfeiffer S, Savarese E, Krug A, Garlanda C, *et al.* Tir8/Sigirr prevents murine lupus by suppressing the immunostimulatory effects of lupus autoantigens. J Exp Med **2008**;205(8):1879-88.

17. Bulek K, Swaidani S, Qin J, Lu Y, Gulen MF, Herjan T, *et al.* The essential role of single Ig IL-1 receptor-related molecule/Toll IL-1R8 in regulation of Th2 immune response. J Immunol **2009**;182(5):2601-9.

18. Nold-Petry CA, Lo CY, Rudloff I, Elgass KD, Li S, Gantier MP, *et al.* IL-37 requires the receptors IL-18Ralpha and IL-1R8 (SIGIRR) to carry out its multifaceted anti-inflammatory program upon innate signal transduction. Nat Immunol **2015**;16(4):354-65 doi 10.1038/ni.3103.

19. Xiao H, Gulen MF, Qin J, Yao J, Bulek K, Kish D, *et al.* The Toll-interleukin-1 receptor member SIGIRR regulates colonic epithelial homeostasis, inflammation, and tumorigenesis. Immunity **2007**;26(4):461-75.

20. Drexler SK, Kong P, Inglis J, Williams RO, Garlanda C, Mantovani A, *et al.* SIGIRR/TIR-8 is an inhibitor of Toll-like receptor signaling in primary human cells and regulates inflammation in models of rheumatoid arthritis. Arthritis Rheum **2010**;62(8):2249-61 doi 10.1002/art.27517.

21. Gulen MF, Kang Z, Bulek K, Youzhong W, Kim TW, Chen Y, *et al.* The receptor SIGIRR suppresses Th17 cell proliferation via inhibition of the interleukin-1 receptor pathway and mTOR kinase activation. Immunity **2010**;32(1):54-66.

22. Russell SE, Stefanska AM, Kubica M, Horan RM, Mantovani A, Garlanda C, *et al.* Toll IL-1R8/Single Ig IL-1-Related Receptor Regulates Psoriasiform Inflammation through Direct

570 Inhibition of Innate IL-17A Expression by gammadelta T Cells. J Immunol **2013**;191(6):3337-46
571 doi 10.4049/jimmunol.1300828.
572 23. Batliwalla FM, Li W, Ritchlin CT, Xiao X, Brenner M, Laragione T, *et al.* Microarray
573 analyses of peripheral blood cells identifies unique gene expression signature in psoriatic arthritis.
574 Mol Med **2005**;11(1-12):21-9.
575 24. Garlanda C, Riva F, Veliz T, Polentarutti N, Pasqualini F, Radaelli E, *et al.* Increased
576 susceptibility to colitis-associated cancer of mice lacking TIR8, an inhibitory member of the
577 interleukin-1 receptor family. Cancer Res **2007**;67(13):6017-21.
578 25. Xiao H, Yin W, Khan MA, Gulen MF, Zhou H, Sham HP, *et al.* Loss of single
579 immunoglobulin interlukin-1 receptor-related molecule leads to enhanced colonic polyposis in
580 Apc(min) mice. Gastroenterology **2010**;139(2):574-85.
581 26. Bertilaccio MT, Simonetti G, Dagklis A, Rocchi M, Rodriguez TV, Apollonio B, *et al.* Lack
582 of TIR8/SIGIRR triggers progression of chronic lymphocytic leukemia in mouse models. Blood
583 **2011**;118(3):660-9 doi 10.1182/blood-2011-01-329870.
584 27. Campesato LF, Silva APM, Cordeiro L, Correa BR, Navarro FCP, Zanin RF, *et al.* High IL-
585 1R8 expression in breast tumors promotes tumor growth and contributes to impaired antitumor
586 immunity. Oncotarget **2017**;8(30):49470-83 doi 10.18632/oncotarget.17713.
587 28. Molgora M, Bonavita E, Ponzetta A, Riva F, Barbagallo M, Jaillon S, *et al.* IL-1R8 is a
588 checkpoint in NK cells regulating anti-tumour and anti-viral activity. Nature **2017**;551(7678):110-4
589 doi 10.1038/nature24293.
590 29. Leadbetter EA, Rifkin IR, Hohlbaum AM, Beaudette BC, Shlomchik MJ, Marshak-
591 Rothstein A. Chromatin-IgG complexes activate B cells by dual engagement of IgM and Toll-like
592 receptors. Nature **2002**;416(6881):603-7.
593 30. Means TK, Latz E, Hayashi F, Murali MR, Golenbock DT, Luster AD. Human lupus
594 autoantibody-DNA complexes activate DCs through cooperation of CD32 and TLR9. J Clin Invest
595 **2005**;115(2):407-17 doi 10.1172/JCI23025.

596 31. Scielzo C, Bertilaccio MT, Simonetti G, Dagklis A, ten Hacken E, Fazi C, *et al.* HS1 has a
597 central role in the trafficking and homing of leukemic B cells. Blood **2010**;116(18):3537-46 doi
598 10.1182/blood-2009-12-258814.
599 32. Fonte E, Agathangelidis A, Reverberi D, Ntoufa S, Scarfo L, Ranghetti P, *et al.* Toll-like
600 receptor stimulation in splenic marginal zone lymphoma can modulate cell signaling, activation and
601 proliferation. Haematologica **2015**;100(11):1460-8 doi 10.3324/haematol.2014.119933.
602 33. Adachi M, Watanabe-Fukunaga R, Nagata S. Aberrant transcription caused by the insertion
603 of an early transposable element in an intron of the Fas antigen gene of lpr mice. Proc Natl Acad Sci
604 U S A **1993**;90(5):1756-60.
605 34. Bichi R, Shinton SA, Martin ES, Koval A, Calin GA, Cesari R, *et al.* Human chronic
606 lymphocytic leukemia modeled in mouse by targeted TCL1 expression. Proc Natl Acad Sci U S A
607 **2002**;99(10):6955-60 doi 10.1073/pnas.102181599.
608 35. Ritchie ME, Phipson B, Wu D, Hu Y, Law CW, Shi W, *et al.* limma powers differential
609 expression analyses for RNA-sequencing and microarray studies. Nucleic Acids Res
610 **2015**;43(7):e47 doi 10.1093/nar/gkv007.
611 36. Subramanian A, Tamayo P, Mootha VK, Mukherjee S, Ebert BL, Gillette MA, *et al.* Gene
612 set enrichment analysis: a knowledge-based approach for interpreting genome-wide expression
613 profiles. Proc Natl Acad Sci U S A **2005**;102(43):15545-50 doi 10.1073/pnas.0506580102.
614 37. Bernasconi NL, Traggiai E, Lanzavecchia A. Maintenance of serological memory by
615 polyclonal activation of human memory B cells. Science **2002**;298(5601):2199-202 doi
616 10.1126/science.1076071.
617 38. De Groof A, Hemon P, Mignen O, Pers JO, Wakeland EK, Renaudineau Y, *et al.*
618 Dysregulated Lymphoid Cell Populations in Mouse Models of Systemic Lupus Erythematosus. Clin
619 Rev Allergy Immunol **2017**;53(2):181-97 doi 10.1007/s12016-017-8605-8.

620 39. Compagno M, Lim WK, Grunn A, Nandula SV, Brahmachary M, Shen Q, *et al.* Mutations
621 of multiple genes cause deregulation of NF-kappaB in diffuse large B-cell lymphoma. Nature
622 **2009**;459(7247):717-21 doi 10.1038/nature07968.
623 40. Ngo VN, Young RM, Schmitz R, Jhavar S, Xiao W, Lim KH, *et al.* Oncogenically active
624 MYD88 mutations in human lymphoma. Nature **2011**;470(7332):115-9 doi 10.1038/nature09671.
625 41. Nogai H, Wenzel SS, Hailfinger S, Grau M, Kaergel E, Seitz V, *et al.* IkappaB-zeta controls
626 the constitutive NF-kappaB target gene network and survival of ABC DLBCL. Blood
627 **2013**;122(13):2242-50 doi 10.1182/blood-2013-06-508028.
628 42. Molgora M, Barajon I, Mantovani A, Garlanda C. Regulatory Role of IL-1R8 in Immunity
629 and Disease. Front Immunol **2016**;7:149 doi 10.3389/fimmu.2016.00149.
630 43. Piva R, Pellegrino E, Mattioli M, Agnelli L, Lombardi L, Boccalatte F, *et al.* Functional
631 validation of the anaplastic lymphoma kinase signature identifies CEBPB and BCL2A1 as critical
632 target genes. J Clin Invest **2006**;116(12):3171-82 doi 10.1172/JCI29401.
633 44. Minguet S, Dopfer EP, Pollmer C, Freudenberg MA, Galanos C, Reth M, *et al.* Enhanced B-
634 cell activation mediated by TLR4 and BCR crosstalk. Eur J Immunol **2008**;38(9):2475-87 doi
635 10.1002/eji.200738094.
636 45. Jiang W, Lederman MM, Harding CV, Rodriguez B, Mohner RJ, Sieg SF. TLR9 stimulation
637 drives naive B cells to proliferate and to attain enhanced antigen presenting function. Eur J
638 Immunol **2007**;37(8):2205-13 doi 10.1002/eji.200636984.
639 46. Li S, Neff CP, Barber K, Hong J, Luo Y, Azam T, *et al.* Extracellular forms of IL-37 inhibit
640 innate inflammation in vitro and in vivo but require the IL-1 family decoy receptor IL-1R8. Proc
641 Natl Acad Sci U S A **2015**;112(8):2497-502 doi 10.1073/pnas.1424626112.
642 47. Clementi R, Dagna L, Dianzani U, Dupre L, Dianzani I, Ciceri F, *et al.* Inherited perforin
643 and fas mutations in a patient with autoimmune lymphoproliferative syndrome and lymphoma.
644 Blood **2004**;104(11):387a-a.

645 48. Sangaletti S, Tripodo C, Vitali C, Portararo P, Guarnotta C, Casalini P, *et al.* Defective
646 Stromal Remodeling and Neutrophil Extracellular Traps in Lymphoid Tissues Favor the Transition
647 from Autoimmunity to Lymphoma. Cancer Discov **2014**;4(1):110-29 doi 10.1158/2159-8290.Cd-
648 13-0276.
649 49. Lim KH, Yang Y, Staudt LM. Pathogenetic importance and therapeutic implications of NF-
650 kappaB in lymphoid malignancies. Immunol Rev **2012**;246(1):359-78 doi 10.1111/j.1600-
651 065X.2012.01105.x.
652 50. Pasqualucci L, Dalla-Favera R. Genetics of diffuse large B-cell lymphoma. Blood
653 **2018**;131(21):2307-19 doi 10.1182/blood-2017-11-764332.
654 51. Qin J, Qian Y, Yao J, Grace C, Li X. SIGIRR inhibits interleukin-1 receptor- and toll-like
655 receptor 4-mediated signaling through different mechanisms. J Biol Chem **2005**;280(26):25233-41.
656 52. Henry CJ, Casas-Selves M, Kim J, Zaberezhnyy V, Aghili L, Daniel AE, *et al.* Aging-
657 associated inflammation promotes selection for adaptive oncogenic events in B cell progenitors. J
658 Clin Invest **2015**;125(12):4666-80 doi 10.1172/JCI83024.
659 53. Kato M, Sanada M, Kato I, Sato Y, Takita J, Takeuchi K, *et al.* Frequent inactivation of A20
660 in B-cell lymphomas. Nature **2009**;459(7247):712-6 doi 10.1038/nature07969.
661 54. Liu Z, Zhang J, Gao Y, Pei L, Zhou J, Gu L, *et al.* Large-scale characterization of DNA
662 methylation changes in human gastric carcinomas with and without metastasis. Clin Cancer Res
663 **2014**;20(17):4598-612 doi 10.1158/1078-0432.CCR-13-3380.
664 55. Zhao J, Bulek K, Gulen MF, Zepp JA, Karagkounis G, Martin BN, *et al.* Human Colon
665 Tumors Express a Dominant-Negative Form of SIGIRR That Promotes Inflammation and Colitis-
666 Associated Colon Cancer in Mice. Gastroenterology **2015**;149(7):1860-71 e8 doi
667 10.1053/j.gastro.2015.08.051.
668 56. Vilia MG, Fonte E, Veliz Rodriguez T, Tocchetti M, Ranghetti P, Scarfo L, *et al.* The
669 inhibitory receptor toll interleukin-1R 8 (TIR8/IL-1R8/SIGIRR) is downregulated in chronic

lymphocytic leukemia. Leuk Lymphoma **2017**;58(10):2419-25 doi 10.1080/10428194.2017.1295142.

57. Campo E, Swerdlow SH, Harris NL, Pileri S, Stein H, Jaffe ES. The 2008 WHO classification of lymphoid neoplasms and beyond: evolving concepts and practical applications. Blood **2011**;117(19):5019-32 doi 10.1182/blood-2011-01-293050.

Figure legends:

Figure 1. IL1R8 deficiency increases the severity of the lymphoproliferative disorder of *lpr* mice.

A) Mortality rate at 15 months of age in *Il1r8*$^{-/-}$*/lpr* mice (100%; n = 23) and in *Il1r8*$^{+/+}$*/lpr* mice (22%; n = 27) (Mantel-Cox test $P<0.0001$). B) Spleen (lower panel) and mandibular lymph nodes (upper panel) from 10-12-month-old *Il1r8*$^{+/+}$, *Il1r8*$^{-/-}$, *Il1r8*$^{+/+}$*/lpr*, *Il1r8*$^{-/-}$*/lpr* mice. C) Spleen weights of 10-12-month-old *Il1r8*$^{+/+}$ (n=6), *Il1r8*$^{-/-}$ (n=6), *Il1r8*$^{+/+}$*/lpr* (n=30), and *Il1r8*$^{-/-}$*/lpr* (n=33) mice (unpaired Student *t* test with Welch's correction; mean and SD are indicated).

Figure 2. IL1R8 deficiency is associated with increased susceptibility to lymphoma development in *lpr* mice.

A, B) Histopathological analysis of the spleen (A) and lymph nodes (B) of 10-12-month-old *Il1r8*$^{+/+}$, *Il1r8*$^{-/-}$, *Il1r8*$^{+/+}$*/lpr*, and *Il1r8*$^{-/-}$*/lpr* mice stained with H&E (400x; Axioskop 40 microscope equipped with AxioCam MRc camera and AxioVision Rel. 4.8 acquisition software; Zeiss). C, D) Pathological score of the spleen (C) and lymph nodes (D) of 10-12-month-old *Il1r8*$^{+/+}$ (n = 2), *Il1r8*$^{-/-}$ (n = 2), *Il1r8*$^{+/+}$*/lpr* (n = 20), *Il1r8*$^{-/-}$*/lpr* (n = 26) mice (unpaired Student *t* test; mean and SD are indicated). E) Incidence of DLBCL in *Il1r8*$^{+/+}$*/lpr* (3/23) and *Il1r8*$^{-/-}$*/lpr* (13/26) mice (Fisher test).

Figure 3. *Il1r8*$^{-/-}$*/lpr* mice develop DLBCL lesions.

Immunohistochemical analysis of: B220 (A), CD3 (B) and Ki67 (C) in the spleen of 10-12-month-old *Il1r8*$^{+/+}$, *Il1r8*$^{-/-}$, *Il1r8*$^{+/+}$*/lpr,* and *Il1r8*$^{-/-}$*/lpr* mice (40x). Immunohistochemical analysis of: bcl-2 (D), bcl-6 (E) and MUM-1 (F) in the spleen of 10-12-month-old *Il1r8*$^{-/-}$*/lpr* mice (Representative images from 5 mice analyzed; 400x; Axioskop 40 microscope equipped with AxioCam MRc camera and AxioVision Rel. 4.8 acquisition software; Zeiss).

Figure 4. DLBCL lesions are transplantable and oligoclonal.

A) Histopathological analysis of the spleen of a 12-month-old *Il1r8*$^{-/-}$*/lpr* donor mice compared to the spleen of *Il1r8*$^{+/+}$ recipient mice stained with H&E(Axioskop 40, Zeiss, 200 and 400x for left and right panels). B) Genomic analysis by PCR of *lpr* and *Il1r8* targeted genes in organs of one recipient mouse 6.5 months after transplantation with *Il1r8*$^{-/-}$*/lpr* spleen and lymph node cells. A, B: Representative images of 1/8 *Il1r8*$^{-/-}$*/lpr* donors and 1/8 recipients in which the transplanted cells generated a lymphoma. C, D) Southern blot analysis of Ig genes shows rearrangement and oligoclonal expansion of B cells in one recipient mouse of *Il1r8*$^{-/-}$*/lpr* spleen and lymph node cells. Genomic DNA from different organs and tissues of the recipient animal was digested with EcoRI (C) or StuI (D). Yellow arrows indicate clonal bands.

Figure 5. Dysregulated NF-κB activation in *Il1r8*$^{+/+}$*/lpr* and *Il1r8*$^{-/-}$*/lpr* mice.

A) Western blot of spleen B cells with the indicated antibodies. β-actin expression was analyzed as internal control. B, C) Densitometric signal ratios of p52/p100 and phospho-p65/p65 shown in panel A (Mann Whitney test; * = *P* value < 0.05). *n* = 4 *Il1r8*$^{+/+}$, *n* = 5 *Il1r8*$^{-/-}$, *n* = 4 *Il1r8*$^{+/+}$*/lpr*, *n* = 6 *Il1r8*$^{-/-}$*/lpr* mice. D) Real-time PCR array of NF-κB signaling target genes. Expression data are shown only for the genes for which a Fold Difference (FD) > 2 was observed in at least one comparison between two groups of mice (see supplementary Table S2 for individual data). In the graph, a two-color scale formatting scheme was used to format cells: red is the maximum expression; blue, minimum. Each column represents one sample (from one mouse). E) Nfkbiz

mRNA expression in purified B cells (unpaired Student *t* test with Welch's correction). A-E: One experiment performed. F) FACS analysis of CD86 expression in overnight cultured purified B cells in basal condition and after LPS stimulation. Upper panels: Representative histograms. Lower panels: Results are reported as MFI normalized on fluorescence minus one. One representative experiment with B cells collected from 3-6 mice (one or 2 replicates per mouse) out of 2 performed is shown (unpaired Student *t* test with Welch's correction). B, C, E, F: mean and SD are shown.

Figure 6. IL1R8 is downmodulated in human lymphoma cell lines.

A) Real-time PCR analysis of IL1R8 mRNA expression (unpaired Student *t* test of each line *vs* normal B cells with Welch's correction; mean and SD are indicated; the highest *P* value is reported) and B) Flow cytometric analysis of IL1R8 protein expression (upper panel: representative histograms; lower panel: MFI quantification) in human lymphoma cell lines compared to circulating B ($CD19^+$) cells from 3-4 healthy donors (unpaired Student *t* test of each line *vs* normal B cells; mean and SD are indicated; the highest *P* value is reported); 3-4 experiments were performed with each cell line. Results are expressed as Arbitrary Units (A) and as MFI normalized on fluorescence minus one (B, lower panel).

C) Normalized log intensity of IL1R8 probe (218921_at; GSE43677) in DLBCL versus normal B cells (naive B cells, germinal center (GC) B cells, post GC B cells, and tonsil samples). D) Normalized log intensity of IL1R8 probe (A_23_P84344; GSE32018) in DLBCL *vs* FL, MCL, MALT, NMZL, CLL and lymph node samples. E) Kaplan-Meier survival curve of DLBCL patients (n = 98) with low and high IL1R8 gene expression (218921_at probe) within DLBCL specimens (HR = 2.2; 95% C.I. 1.2-3.8; *P* = 0.006).

Figure 1

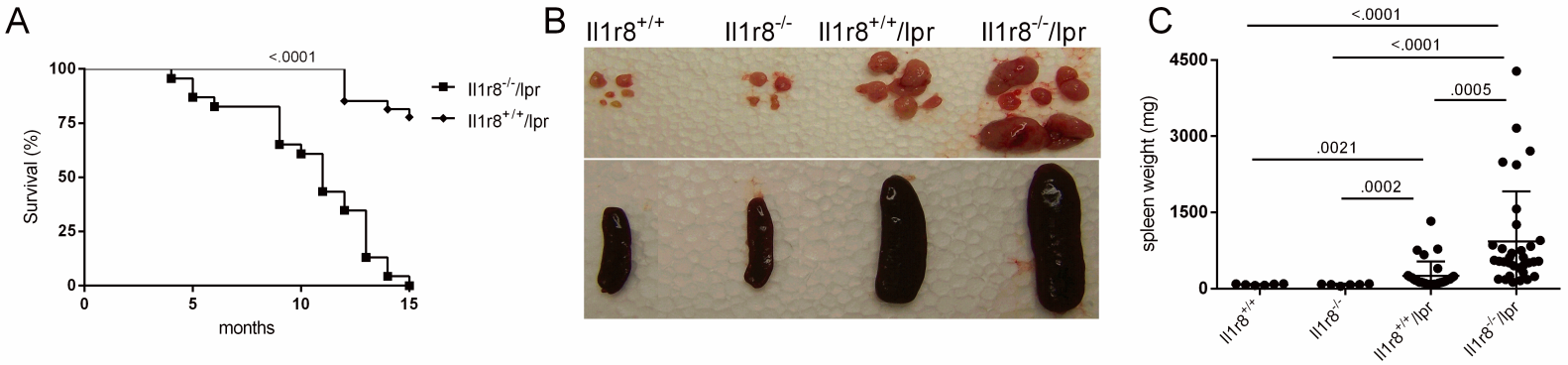

Figure 2

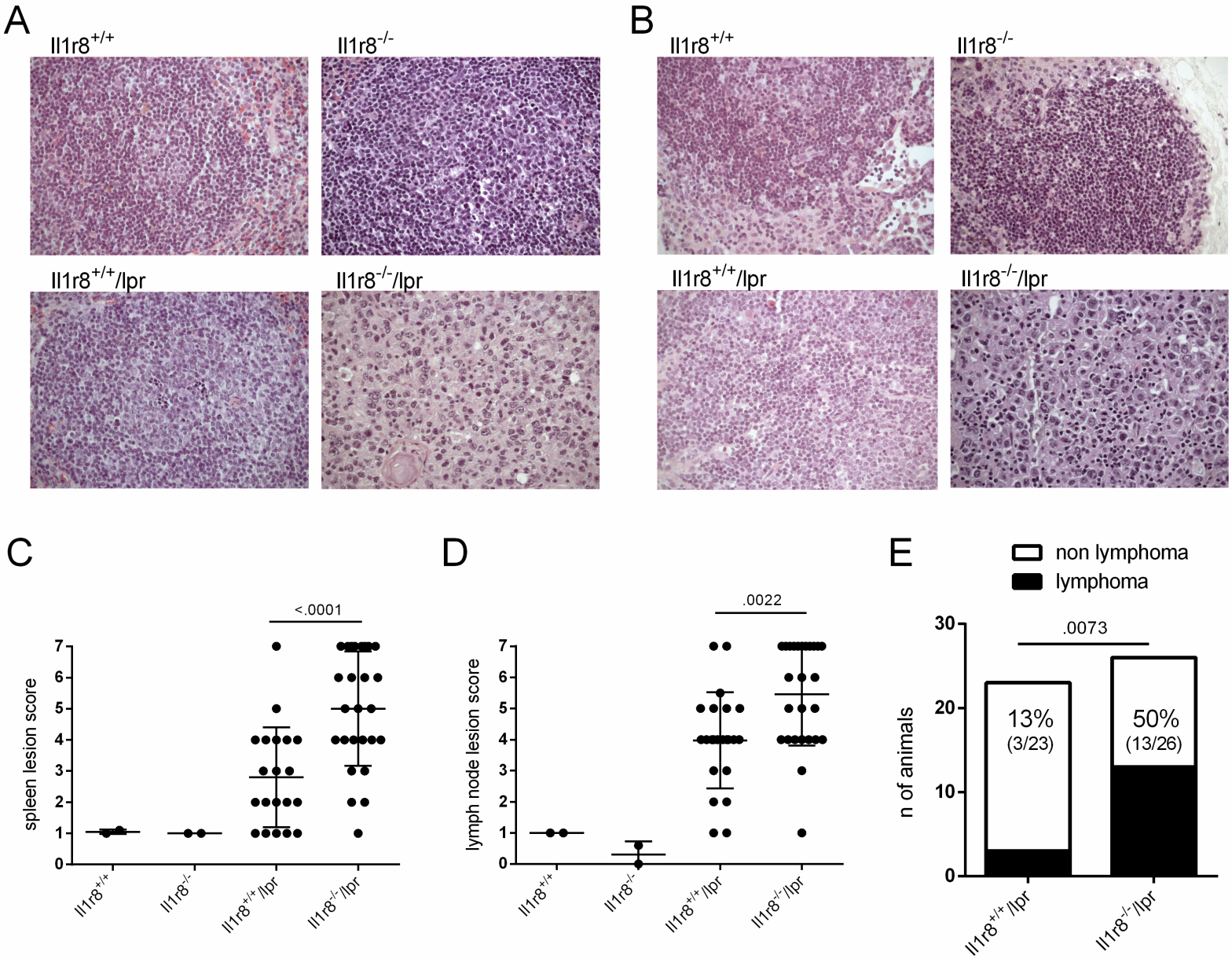

Figure 3

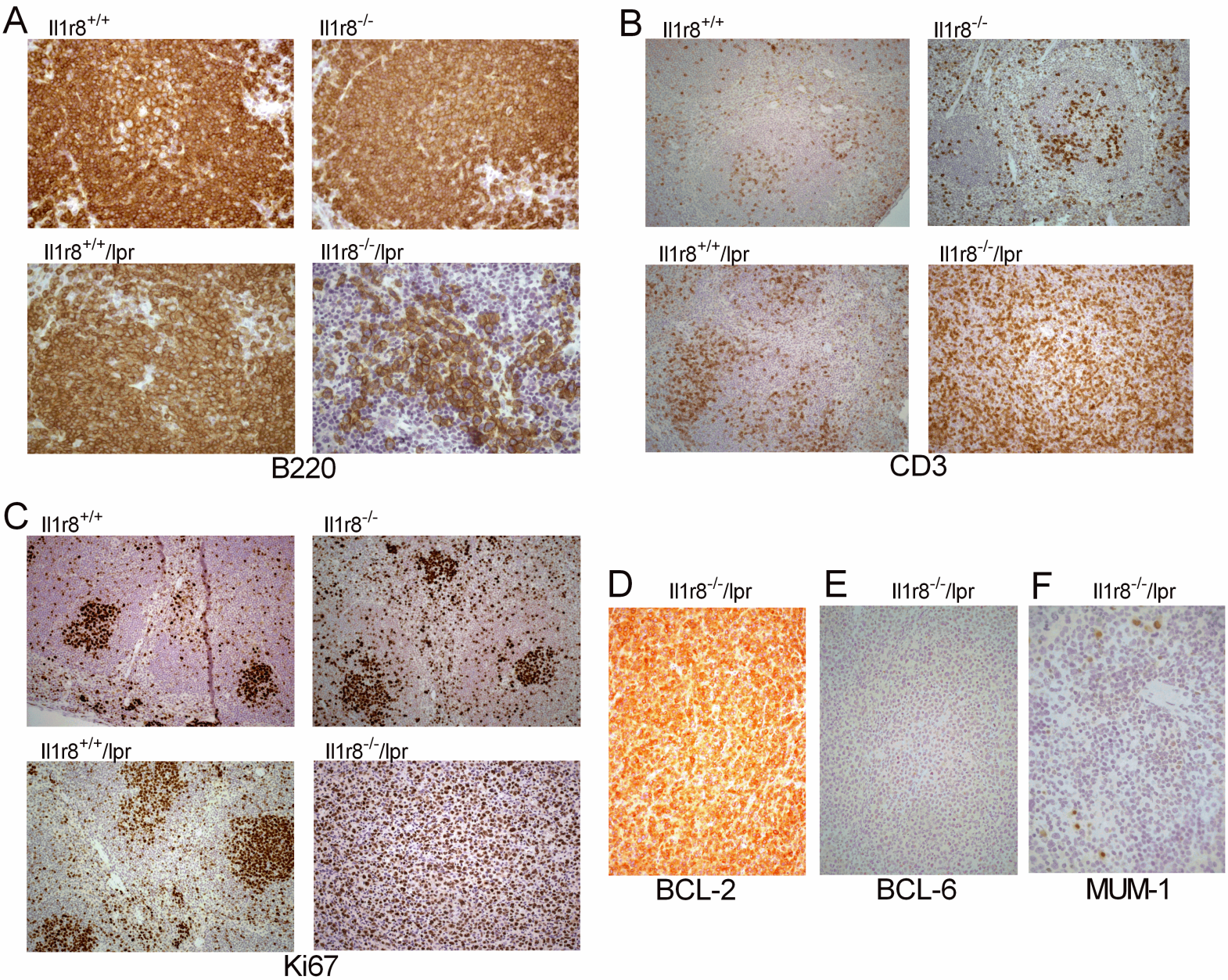

Figure 4

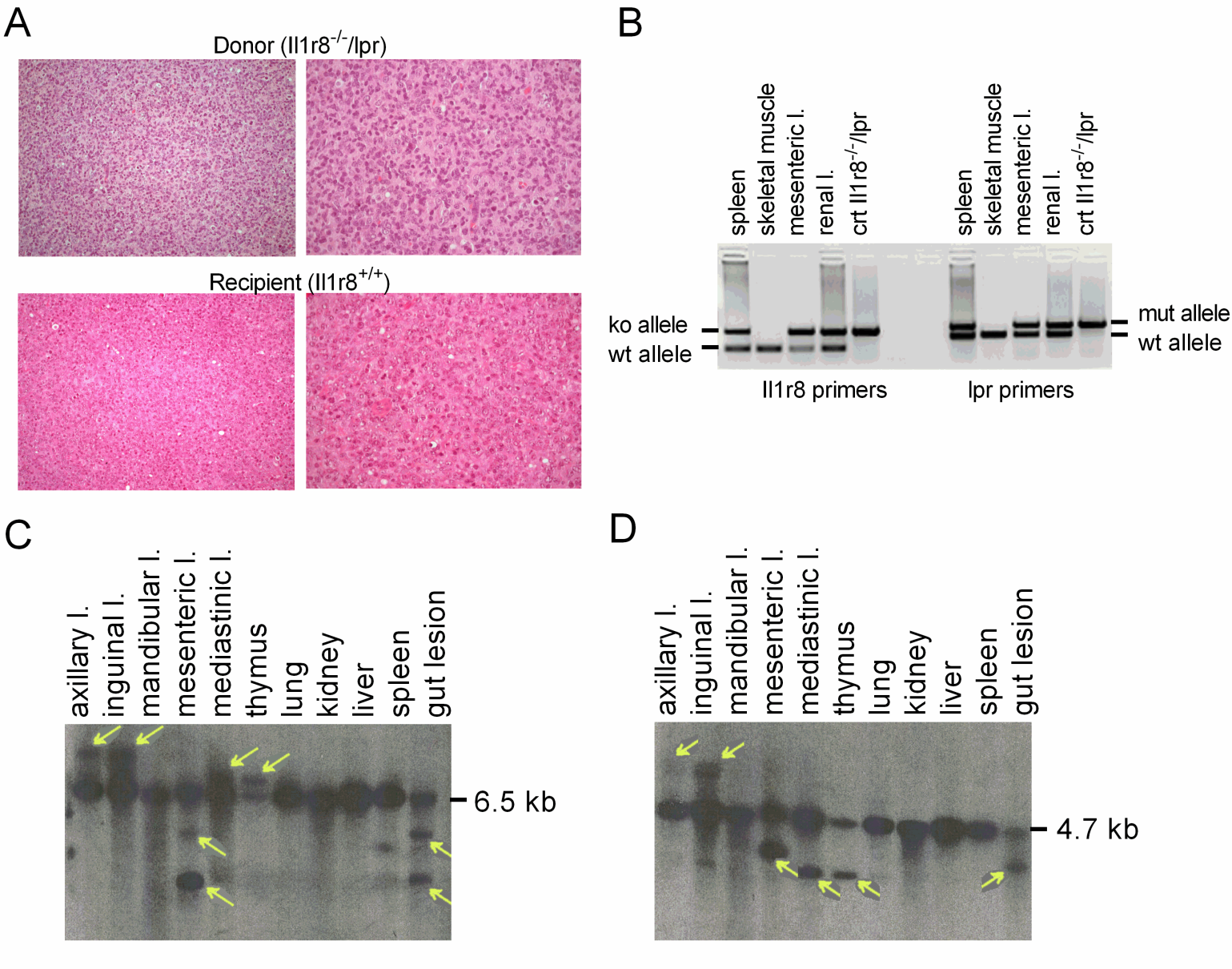

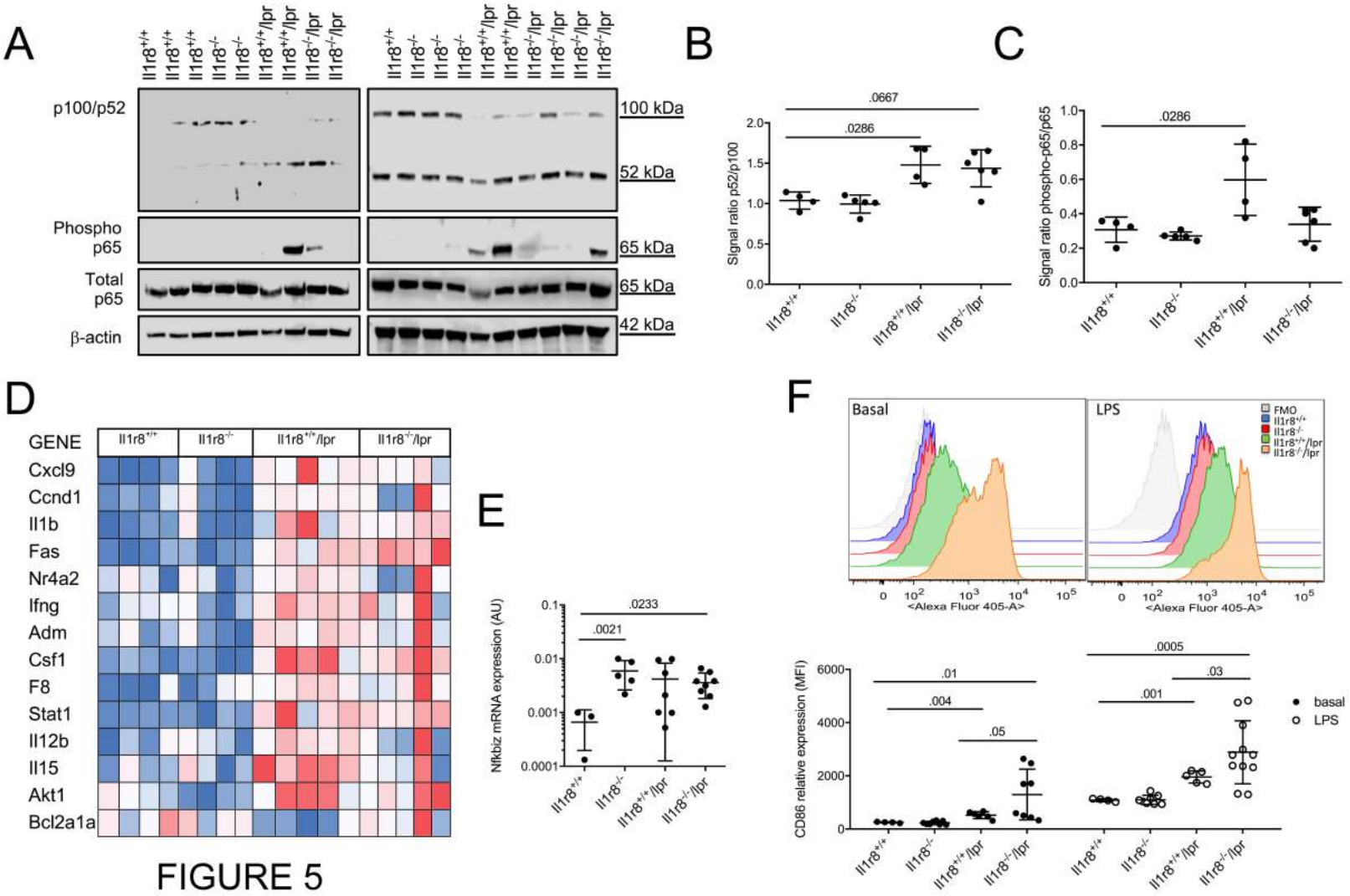

FIGURE 5

FIGURE 6

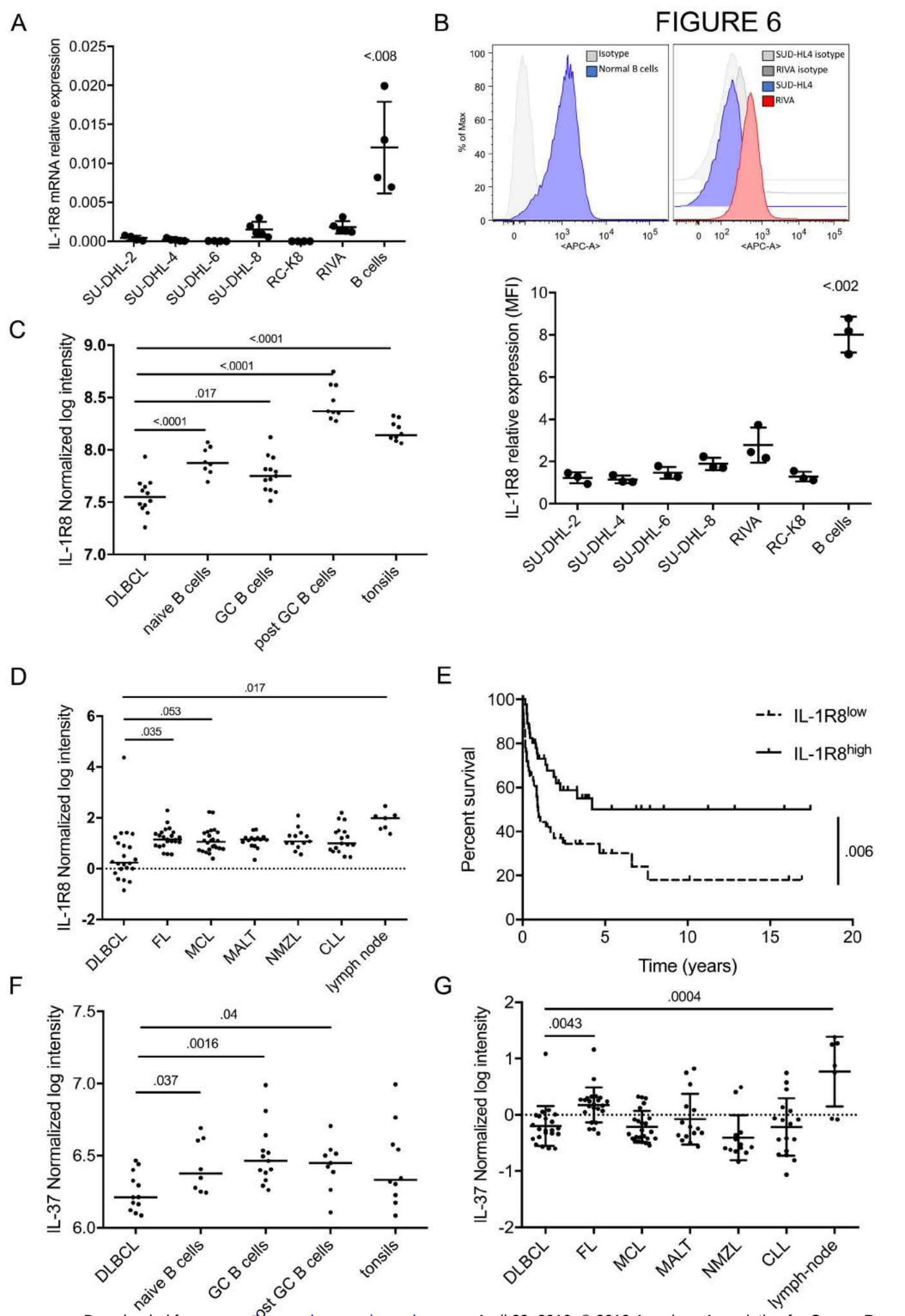

AACR American Association for Cancer Research

Cancer Immunology Research

IL1R8 DEFICIENCY DRIVES AUTOIMMUNITY-ASSOCIATED LYMPHOMA DEVELOPMENT

Federica Riva, Maurilio Ponzoni, Domenico Supino, et al.

Cancer Immunol Res Published OnlineFirst April 24, 2019.